Cycloreversion in Metal-Assisted Olefin Oxidation by Peroxide. Molybdenum(VI) vs. Rhodium(III)

Keith F. Purcell

Department of Chemistry, Kansas State University, Manhattan, Kansas 66506

Received July 10, 1984

Cycloreversion of C_2H_4O from a peroxometallocyclic ring, $L_nM(C_2H_4O_2)$, is compared for M = Mo(VI) and M = Rh(III). The adiabatic ground-state surfaces for concerted cycloreversion give no basis for explaining why M = Mo(VI) produces epoxide while M = Rh(III) fails to do so, producing instead a carbonyl oxidation product. Examination of the frontier orbital energies, however, suggests nonadiabaticity for the M = Rh(III) reaction and also indicates nonconcerted ring opening is likely for M = Rh(III). Bond breaking during cycloreversion for M = Mo(VI) can be depicted as Mo–C electron pair transfer to the O–O σ^* orbital, whereas for M = Rh(III) electron pair transfer to O–O σ^* is initially from a Rh d π orbital. The study also identifies the possible occurrence of an isomerized metallocycle intermediate, $L_nM(OC_2H_4O)$, as well as questions the significance of a four-membered ring structure, $L_nM(O)(C_2H_4O)$, in the oxidation processes.

Introduction

An interesting aspect of metal-assisted oxidation of olefins by peroxide is the effect of a change in the metal on the nature of the oxidation product: with Mo(VI), a d^0 case, epoxide appears as the initially formed product,[1] with Pt(II), a d^8 case, a five-membered peroxoplatinocycle intermediate can be isolated for fully substituted olefins;[2] with Rh(III), a d^6 case, an aldehyde or ketone, depending on the olefin, is produced when the olefin (ol) is not fully substituted.[3-7]

$$OMo(O_2)_2L_2 + ol \rightarrow epoxide + Mo\ product \quad (1)$$

$$PtL_2(O_2) + ol \rightarrow L_2Pt(OC_2R_4O) \quad (2)$$

$$RhL_4(O_2) + ol \rightarrow aldehyde + Rh\ product \quad (3)$$

Aside from peripheral changes in metal coordination number when Mo(VI) is replaced by Rh(III), there are fundamental changes in the number of occupied metal orbitals and in their energies which might provide insight into the reasons for different oxidation products for the two metals.

In earlier work we investigated the electronic features of antrafacial cycloreversion of epoxide from an assumed five-membered ring intermediate (1), the ring skeleton

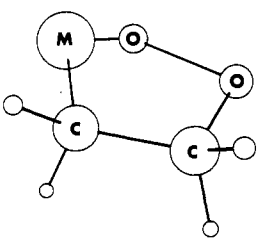

1

being composed of Mo(VI), two oxygen, and two carbon atoms.[8] Key findings findings from that study were that (i) an empty metal dπ atomic orbital suppressed the barrier to cycloreversion by mixing with the lower lying HOMO (the Mo–C bond) so as to partially preserve the Mo–C interaction, (ii) another empty metal dπ atomic orbital also played a key role in suppressing the barrier to cycloreversion by acting as the receptor of the O–O σ bond pair, with formation of the Mo–O(terminal) π bond in the product, and (iii) the reaction proceeds by transfer of the Mo–C electron pair into the O–O σ^* orbital, thereby accomplishing the formation of the new C–O σ bond of the epoxide while rupturing the Mo–C and O–O bonds.

These findings naturally raise the questions: (i) what are the consequences if the metal dπ atomic orbitals are occupied and (ii) what if these metal atomic orbitals are lower lying? These issues are directly encountered when one contemplates a change of metal from Mo(VI) to Rh(III). In this report we wish to extend the studies of peroxometallocyle cycloreversion to Rh(III). Specifically, we compare cycloreversion of $C_2H_4O_2$ from $(H_3P)_3Rh(C_2H_4O_2)$ (2) with that from $(O)(O_2)Mo(C_2H_4O_2)$ (3). We find that both (i) and (ii) open the door to formation of a carbonyl oxidation product, rather than of epoxide.

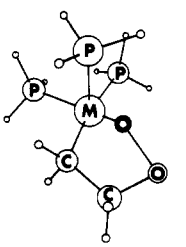

2

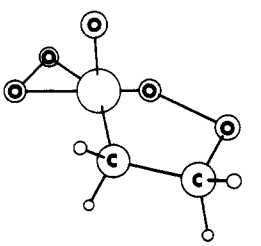

3

Mechanistic Background

The experimental studies of Read,[4] and Mares,[6] and of Mimoun,[1,3,5,7] reviewed and integrated by Mimoun,[9-11] reveal the following common features of metal-assisted olefin oxidation by peroxide.

(a) The peroxometal substrate must possess a vacant coordination site for coordination of the olefin.[7,11] If necessary, ligand dissociation to produce a coordinatively unsaturated metal center is the first step of the reaction.

(b) Coordination of the olefin to the metal is succeeded by insertion of the olefin into a metal–oxygen(peroxo) bond. This produces the five-membered peroxometallo-

(1) H. Mimoun, I. Serée de Roch, and L. Sajus, *Tetrahedron*, **26**, 37 (1970).
(2) R. A. Sheldon and J. A. Van Doorn, *J. Organomet. Chem.*, **94**, 115 (1975).
(3) F. Igersheim and H. Mimoun, *J. Chem. Soc., Chem. Commun.*, 559 (1978).
(4) C. Dudley and G. Read, *Tetrahedron Lett.*, 5273 (1972); C. Dudley, G. Read, and P. J. C. Walker, *J. Chem. Soc., Dalton Trans.*, 833 (1977), M. T. Atley, M. R. Graham, K. Kite, K. Moss, and G. Read, *J. Mol. Catal.*, **7**, 31 (1980).
(5) H. Mimoun, M. M. Perez-Machirant, and I. Serée de Roch, *J. Am. Chem. Soc.*, **100**, 5437 (1978).
(6) R. Tang, F. Mares, N. Neary, and D. E. Smith, *J. Chem. Soc., Chem. Commun.*, 274 (1979).
(7) F. Igersheim and H. Mimoun, *Nouv. J. Chim.*, **4**, 161 (1980).
(8) K. F. Purcell, *J. Organomet. Chem.*, **252**, 181 (1983).
(9) H. Mimoun, *J. Mol. Catal.*, **7**, 1 (1980).
(10) H. Mimoun, *Angew. Chem., Int. Ed. Engl.*, **21**, 734 (1982).
(11) P. Chaumette, H. Mimoun, L. Saussine, J. Fischer, and A. Mitschler, *J. Organomet. Chem.*, **250**, 291 (1983).

0276-7333/85/2304-0509$01.50/0

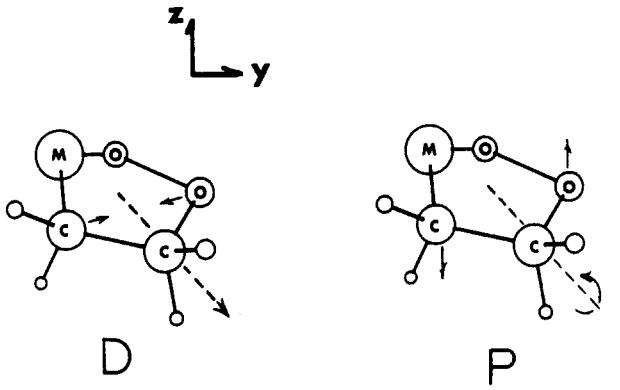

Figure 1. Illustrations of the two independent basis coordinates for the cycloreversion elimination of epoxide from a five-membered peroxometallocycle ring. *D* is the displacement coordinate which is defined as the position of the CH_2CH_2O fragment along the CCO bisector; for each displacement of the fragment along the bisector by 5 pm, the CCO angle closes symmetrically by 2.56° and the CH_2 plane of the terminal methylene pivots by 1.28° about the normal to the CCO plane passing through the terminal carbon. *P* is the dihedral angle defined by the rotating CCO plane and the initial peroxometallocycle plane (*xy*); the CCO rotation axis is the CCO bisector.

cycle from which elimination of the oxidized olefin is to proceed.

(c) In cases where there is a choice, it appears that regiospecificity operates: presumably it is the insertion step which is favored greatly when the M–ol skeletal and M–OO planes are coincident, rather than mutually perpendicular. For example, with the Mo(VI) pentagonal-bipyramidal complexes studied to date, olefin oxidation is unrealized if the olefin is required to occupy an axial coordination site (**4**), as opposed to an equatorial site (**5**). Although this

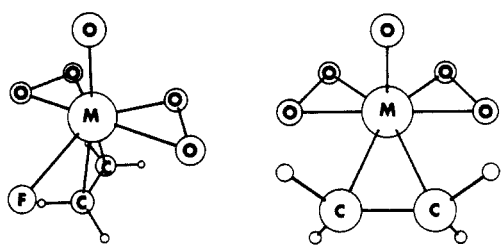

4

5

aspect of the reaction has yet to be subjected to an orbital analysis, it is evident that the insertion step must directly involve the Mo–O bond pair for the equatorial precursor structure, whereas the insertion by an olefin from the axial position will involve both the Mo–O bond pair and pπ lone pair at the oxygen. One may speculate that the barrier to insertion in this latter case is due to weak mixing of the virtual and occupied orbitals required to cleave the Mo–O bond, but there is also the complication that the peroxomolybdocycle produced from this geometry is structurally strained (or, alternately, that to avoid strain within the five-membered ring requires unfavorable electronic changes elsewhere in the molecule). Interestingly, our earlier calculations revealed axial coordination to be thermodynamically favored for the olefin.

Calculational Details

In order to model the cycloreversion reaction coordinate, it is necessary to assume a coordination geometry for the peroxorhodocycle. Knowing that dissociation of a ligand from L_4RhO_2 (**6**) is required for the reaction to proceed, one is led to a five-coordinate intermediate for the peroxorhodocycle $L_3Rh(O_2C_2H_4)$. The structure of this intermediate is most assuredly square-based pyramidal;[12] one

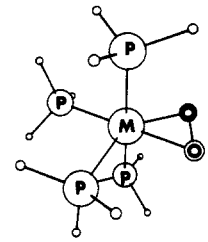

6

has a choice then between facial (**7**) and meridional (**8**) (two

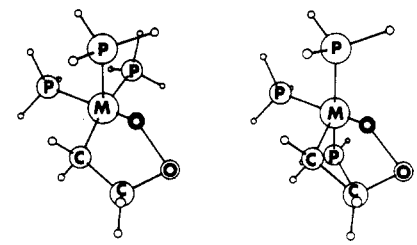

7 **8**

diastereomers) dispositions of the three L ligands. Cycloreversion by the rotation of the CCO fragment is expected to be inhibited in the meridional structure, whereas the facial isomer is characterized by a vacant coordination site disposed so as not to obstruct the pivoting of the Rh–C bond. Accordingly, we have examined the rotatory dissociation of CCO from the facial isomer as the reactive intermediate. We have no disposition at this time as to how this isomer might arise, or even whether this isomer can be realized in practice. For the moment we are interested only in making a comparison of cycloreversion from $RhC_2H_4O_2$ under the constraints which, as nearly as possible, apply to $MoC_2H_4O_2$. The Appendix gives the details of the assumed structure of this intermediate, with L = PH_3.

To describe the essentials of the dissociation of the CCO fragment would require the use of a minimum of five independent basis internal coordinates: the Rh–C and O–O distances, the C–C–O bond angle (alternatively, the C–O distance), the angle between the CH_2 plane at the terminal carbon and the CC axis, and the dihedral angle defined by the basal and CCO planes. Such a moderately complete analysis of the potential surface would be prohibitively expensive and is of questionable merit when the goal of the study is to determine the basic principles of orbital topological control of the reaction. Accordingly, we have simplified the reaction coordinate to a function of two basis internal degrees of freedom. With the peroxometallocycle lying in the *xy* plane, we select as one basis coordinate the position of the central carbon along the bisector of the CCO angle (displacement, *D*); coupled to this coordinate for the CCO fragment are the CCO angle (α), such that $d(\alpha)/d(D)$ = 2.56°/5 pm, and the terminal CH_2 plane/CC axis angle, such that this angle opens 1.28° for each 5 pm change in *D*. In this way dissociation of the CCO fragment (bond breaking) is accompanied by closure of the epoxide ring (bond making), all skeletal motions occurring in the *xy* plane. The second, independent basis coordinate is the CCO plane/*xy* plane dihedral angle (psi, *P*). These basis coordinates are shown in Figure 1; Figure 2 gives pictorial representations of the starting structure (see Appendex for details) and those for displacement along the independent basis coordinates *D* and *P*.

(12) K. F. Purcell and J. C. Kotz, "Inorganic Chemistry", W. B. Saunders, Philadelphia, 1977, p 588.

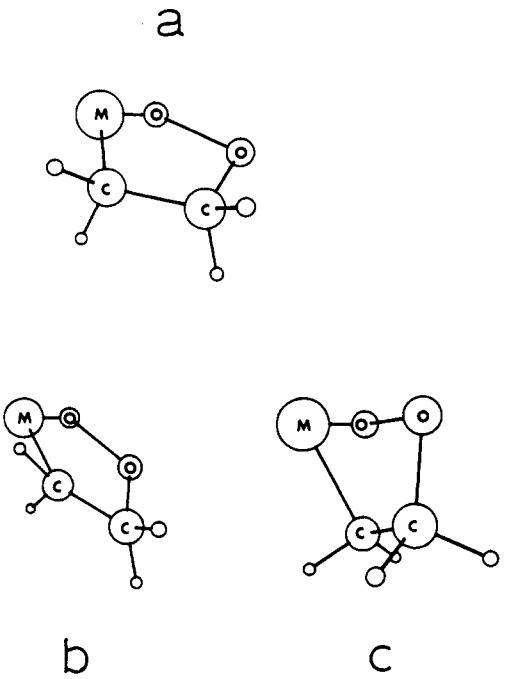

Figure 2. (a) The initial peroxometallocycle ring structure (D = 0 pm; P = 0°). (b) After displacement of the CH_2CH_2O fragment by 60 pm along the CCO bisector (D = 60 pm; P = 0°). (c) After rotation of the CH_2CH_2O fragment by 70° about the CCO bisector (D = 0 pm; P = 70°).

Results and Conclusions

One of the results of the computation, that of the total electronic energy at fixed intervals along D and P, can be best summarized by contour and perspective plots of the energy surface in the domains of D and P. Figure 3 shows the results for both Mo and Rh. There are several significant features in these surfaces.

The starting structures, with planar peroxometallocycle rings, are close to a local minimum (A) with a canted ring structure. Probably the most striking feature of the energy surfaces for both Mo(VI) and Rh(III) is the deep well (B) encountered at P = 180° for the isomerized five-membered ring in which the original O–O and M–C bonds are replaced by O–C and M–O bonds. This result is not unexpected, given the greater bond energies of C–O and M–O linkages relative to O–O and M–C linkages. From a coordination chemist's point of view, the original metallocycle can be viewed as bidentate ligation of the metal by the remarkable "ethyleneperoxidate" ligand, whereas the isomer entails ligation by ethylene-1,2-diolate.

The second significant feature is that there are activation barriers along both D (D = 50 pm; P = 0°) and P (D = 0 pm; P = 50°), that along D being significantly higher than that along $P > 0$, but less than that along $P < 0$ (Rh(III) case). (That the barrier along $P < 0$ is so large confirms our expectation that elimination from the *mer* isomer is strongly inhibited.) The appearance of a col (marked C in Figure 3) between these maxima emphasizes the significant reduction in the CCO elimination barrier when the trajectory entails well-developed CCO rotation. Continuation of the molecule along a CCO dissociative trajectory (A → C → D) takes the molecule through a second col (D in Figure 3) and culminates in elimination of epoxide.

A third observation is that passage to the first col requires less energy for the Rh molecule (35 kJ/mol) than for its Mo analogue (55 kJ/mol). Epoxide, of course, is the observed product for Mo(VI) but is not the product realized in the reaction with Rh(III)!

Our first important conclusion must be that adiabatic cycloreversion to form epoxide is possible (to be distinguished from probable) for both Mo(VI) and Rh(III); that is, failure to observe epoxide as a product from the Rh reaction cannot be ascribed to a higher classical barrier in that case.

A second especially intriguing conclusion is that the same col (C) serves as portal to both epoxide elimination (A → C → D) and isomerization (A → C → B) of the metallocycles. That there has never been experimental detection of the more stable isomerized ring in any MC_2O_2 metallocycle suggests (a) that the trajectory for the reaction is not simply that of steepest descent or (b) that other undetected intermediates may preceed CCO elimination from [...$M(C_2H_4O_2)$] (see below).

Clearly there are features of the elimination reaction which are masked in the Rh(III) case by the gross features of the adiabatic energy surface and the reaction coordinate defining it. To identify these features, we will next examine the orbital topology and orbital energy features of both complexes, looking for possible impediments to passage through col C and/or a harbinger of a lower energy CCO elimination reaction coordinate in the case of Rh(III).

To better understand the bond breaking process brought on by CCO rotation, Figures 4 and 5 are given as summaries of the variation with P of the frontier orbital energies of the metallorhodocycles. At P = 0°, the eigenvectors reveal the highest cycle frontier MO is the OO σ^* MO (OO*) for both complexes. [The next most stable MO is not a ring MO: the axial PRh σ^* (Rh) or the O_2^{2-} ligand π^* MO (Mo).] The lower four frontier orbitals are, in order of increasing stability, the set of metal dπ orbitals (yz, xz, and xy) and the CM σ MO (CM). These are all occupied for M = Rh(III), but only the lowest (CM) is occupied for M = Mo(VI).

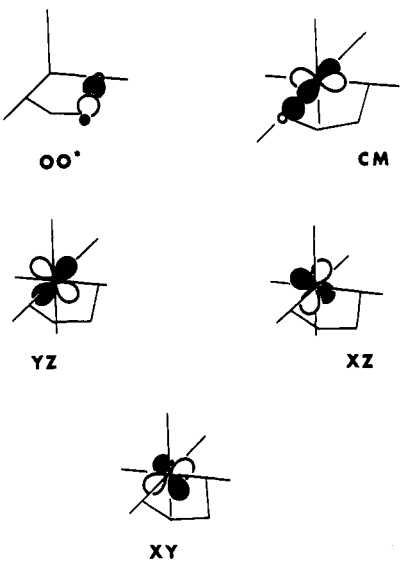

Again from the eigenvectors, the ultimate fate of these orbitals, at P = 90°, are as follows: the RhP σ^* and O_2^{2-} MO's emerge little changed, as do the metal dπ orbitals; the net direct chemical transformation is of CM to an O lone pair (which dissociation transforms into the new ring CO bond).

The twisting motion of the CCO skeleton rotates the ring OO* and the CM MO's out of the xy plane, the former in the $+z$ direction and the latter in the $-z$ direction. The principle effect on the energies of the frontier levels is a sharp plummeting (as the OO distance increases) of the OO σ^* MO to meet its destiny to convert CM into the O lone pair, with attendent (avoided) crossings by this MO

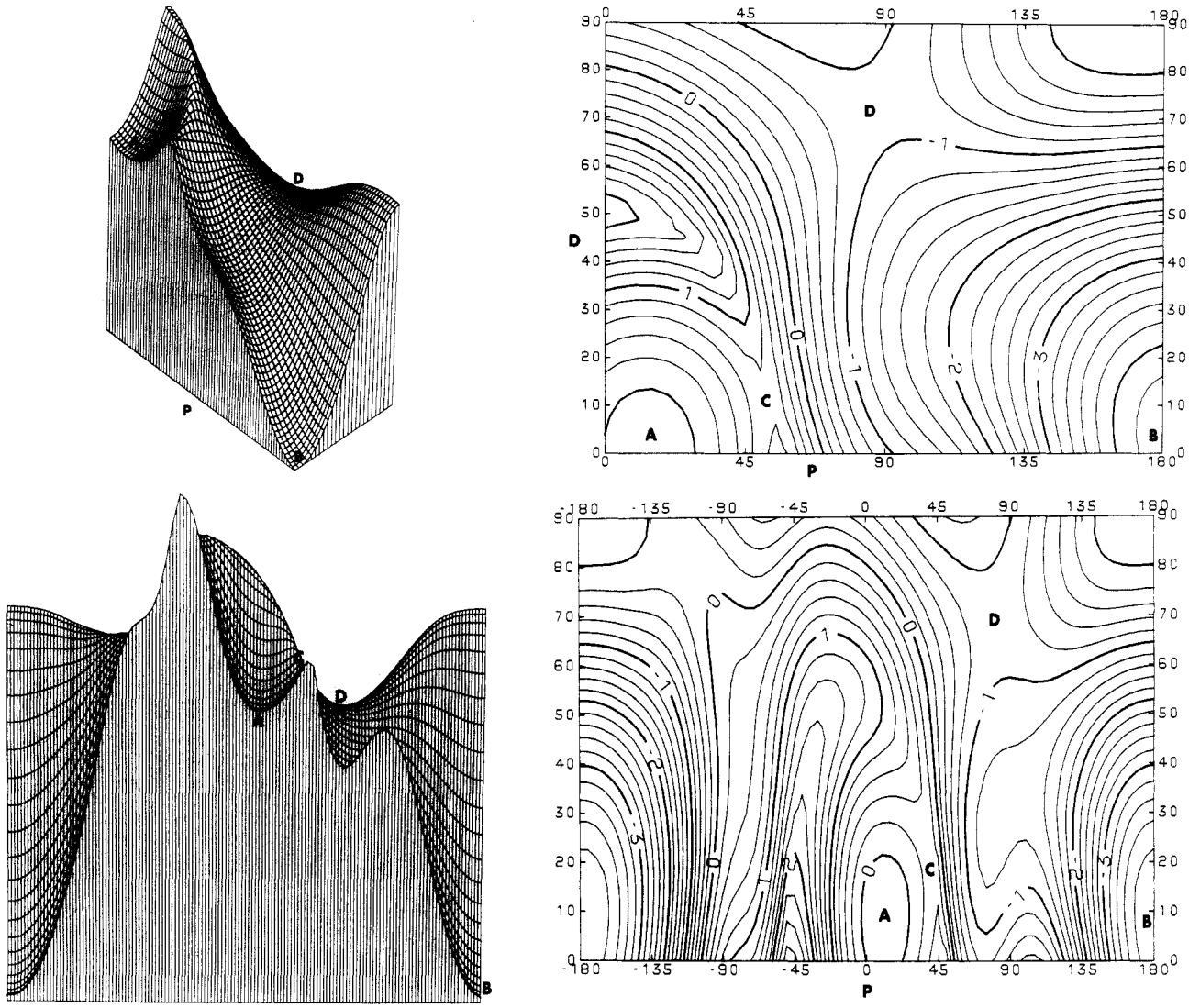

Figure 3. Shown are contour representations and three-dimensional representations of the ground-state energy surfaces for cycloreversion of epoxide from $M(C_2H_4O_2)$ for M = Mo(VI) (top) and Rh(III) (bottom). The surface for Mo(VI) is limited to P in the range 0° through 180°; for Rh(III), the range in P is −180° through 180°.

of the lower lying orbitals. The CM orbital, owing to its position below, and mixing with, the dπ set, remains relatively constant in energy. The first crossing of OO* (at P = 20–30°) with RhP σ*, or O_2^{2-}, is of little chemical consequence as both MO's are virtual. From this point on there are significant differences in the Rh and Mo cases.

For Mo(VI) the dπ MO's are unoccupied, so there is no major development of electron flow as OO* plunges through the dπ levels. The latter become strongly hybridized through their mutual overlap with the rotating C (overlaps xz,xy) and O (overlaps xy,yz) AO's. Because of the energy gap difference for OO*/dπ vs. CM/dπ, it is the xy,yz mixing which is most pronounced, xz being less perturbed (notice in Figure 4 that the original xz level does not show the curvature associated with a strongly avoided crossing with OO*. The rotational barrier at P = 60° corresponds to consumation of the ring opening by the strongly avoided crossing of OO* with CM at P = 55°, where there is transfer of 1.5 e from the M,C atom pair to the O,O atom pair. That this transfer effects nearly synchronous cleavage of the CMo and OO bonds is revealed by the overlap population changes of 0.45 → 0.07 for CMo and 0.24 → −0.10 for OO, as P changes from 50° to 70°.

The Rh(III) case strongly contrasts with that of Mo(VI) by virtue of the facts that the dπ orbitals are occupied, lie much closer to the CM orbital, and lie at energies much like that of CMo. The latter characteristic would have produced a LUMO/HOMO crossing at P = 55° too, were it not for the symmetry breaking nature of P and the proximity of the dπ set to CM in the Rh(III) case: the complex dπ hybridization is complicated by the mixing also with the CRh orbital, producing a rise in the dπ HOMO energy. The first difference for Rh(III), then, is that the LUMO/HOMO crossing thus occurs somewhat earlier, at P = 45°. Note that this crossing corresponds closely to the barrier position (Figure 3).

A second potentially chemically important difference for Rh(III) is that the LUMO/HOMO crossing is weakly avoided this time, owing to the dπ nature of the HOMO. This is such an important feature that its origin was traced as follows. The $-z$ displacement of C as the CCO rotation develops causes mixing of xz with CM, the latter being due mainly to $x^2 - y^2$/C p overlap. The mixing of xz and yz into CM (constructive wave interference) is what maintains the CM bonding in the early stages of the reaction by directing a d AO to track the C atom movement. The counterpart mixing of CM into xz (destructive wave interference) gives CM antibonding character to the initial xz MO, which consequently rises and intends to cross the original yz MO. That crossing is strongly avoided through dπ mixing so that HOMO starts out as yz but takes on

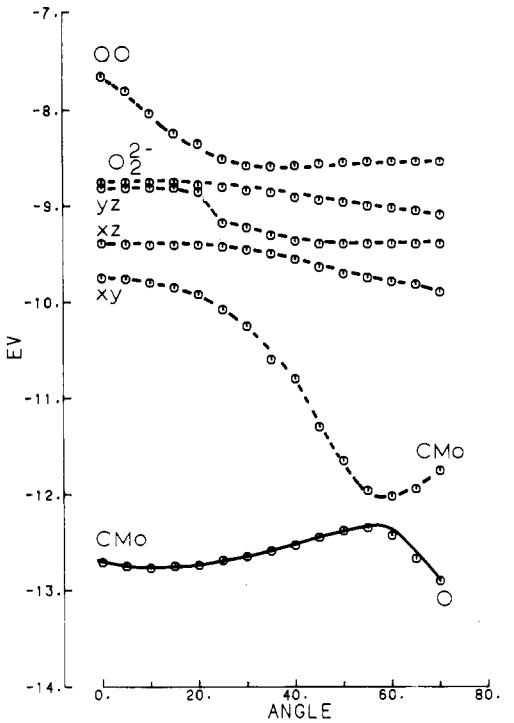

Figure 4. The frontier orbital energies for the Mo(VI) case as functions of P from 0° through 70°. The solid line designates the occupied frontier MO, HOMO in this case.

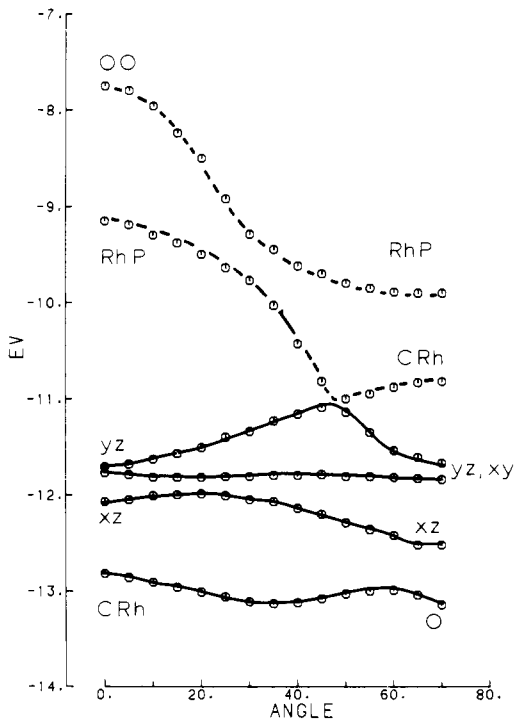

Figure 5. The frontier orbital energies for the Rh(III) case as functions of P from 0° through 70°. Solid lines identify the occupied MO's.

considerable xz AO character as well. Thus at the LUMO/HOMO crossing the HOMO yz content becomes dominated by xz character, and, consistently with the Mo(VI) case, there is a weakly avoided OO*/"xz" crossing. To complete the story, this dπ hybridization, which progressively develops as the transition state is approached, is "undone" beyond the transition state, so as to restore the starting dπ levels.

A third, extremely important difference occasioned by the change in metal concerns the nature of the molecular electron flow at the P = 45° barrier. While there is a net transfer of 1.6 e from the C,M atom pair to the O,O atom pair (much like the Mo(VI) case), this density loss is mainly from Rh (1.1 e) [specifically from the dπ AO's (0.8 e) which play in HOMO a mixed nonbonding (xy,yz)/CM antibonding (xz) role] and *not* from the CRh bond: the CRh and OO overlap population changes are 0.45 → 0.36 and 0.30 → −0.22, respectively, for P = 30–50°. In sharp contrast with the Mo(VI) case, there clearly is *not* synchronous CRh/OO cleavages at the rotational barrier, but dπ → OO* electron transfer to cleave the OO bond well before the CRh bond is cleaved. The latter is not consummated until P = 65°, corresponding to the characteristically strongly avoided crossing of the two lowest, *occupied* frontier orbitals at that point. In this region there is completion of charge flow from C to Rh, as reflected in the transfer of ca. 0.5 e from C to Rh and little change in the O,O pair density (only a loss of 0.1 e). The electron flow C → Rh is mainly into the xz and xy AO's (0.5 e), restoring most of the 0.6 e lost earlier by these two AO's to OO* at the P = 45° barrier.

Summary and Extensions

Two critical points emerge from this study. First, even though epoxide eliminations for the molybdocycle and the rhodocycle appear very similar from the global view of adiabatic potential energy surfaces, even easier for Rh, it is not apparent from these surfaces that the ground-state surface is well separated from the lowest excited state surface at the first col for Mo but not well separated for Rh. This raises the interesting possibility that the reaction rate constant for epoxide elimination is severely depressed by a high probability for nonadiabatic (chemically unproductive) traversal of the col C region.

Second, a sharp contrast in electron flow and bond breaking/making for the two cycles becomes apparent at the orbital level. For Mo, electron transfer from the metal–carbon bond to the peroxo group characterizes development of the reaction along the dissociative coordinate and naturally leads to epoxide formation. For Rh, the electron flow tracking the CCO rotation is quite different; the rotational barrier derives from metal to peroxo transfer to break the OO bond, while the metal–carbon bond is maintained. Thus, the metal–carbon to peroxo electron transfer which facilitates epoxide ring closure for Mo is not found for Rh. This change in electron following of the rotational CCO motion with change in metal is directly linked to the availability of dπ electron pairs at Rh(III), and not for Mo(VI), and to the fact that the metal dπ levels are more closely lying to the metal–carbon bond orbital in the Rh case. It is to be expected that these fundamental differences are directly responsible for the very different olefin oxidation products found for the two metals.

The Rh-to-peroxo electron flow on ring twisting is intriguing in that it suggests asymmetric peroxorhodocycle ring opening is more facile than concerted elimination of epoxide. A dangling ligand intermediate [...$RhC_2H_4O^-$] (**9**) affords the possibility for 1,2-H migration, with return of an electron pair to Rh and elimination of acetaldehyde. Another possibility is that a four-membered ring intermediate [...$Rh(C_2H_4O)$] (**10**) is achieved by coordination of the free oxygen atom of the dangling ligand to the vacant coordination site of Rh or, more directly, by 1,2 migration of the CCO oxygen atom to that site. Aldehyde elimination from this intermediate could then occur by one of several possible paths (1,2-H migration with Rh–C cleavage, β-elimination, etc.).

Finally, the appearance of deep wells in the energy surfaces for the "diolate" metallocycles is expected, but of unknown mechanistic consequences. We must leave open

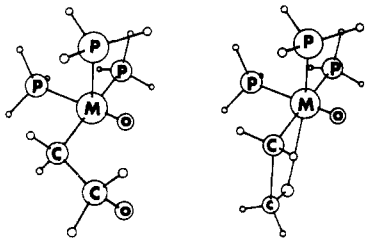

9 10

at this time the possibility that aldehyde formation proceeds from this structure via an MOC_2H_4O– dangling and/or four-membered ring, intermediate. Such an intermediate would be consistent with the delayed formation of aldehyde in the Mo(VI) system:[11]

$$(O_2)(O)Mo(O_2C_2H_4) \rightarrow (O_2)(O)MoO + C_2H_4O$$

$$(O_2)(O)Mo(O_2C_2H_4) \rightarrow (O_2)(O)Mo(OC_2H_4O) \rightarrow (O_2)(O)MoO + CH_3CHO$$

Acknowledgment is made to the donors of the Petroleum Research Fund, administered by the American Chemical Society, for partial support of this research. Support from the National Science Foundation and from the Kansas State University Computing Center is also appreciated.

Appendix

The extended Hückel method, modified for the use of double exponent radial functions, was employed.[13] The starting structural parameters for $(H_3P)_3Rh(C_2H_4O_2)$ are as follows: Rh–P = 228 pm; P–H = 142 pm; Rh–C = 200 pm; C–C = 154 pm; C–O = 147 pm; O–O = 145 pm; Rh–O = 180 pm; all PRhP and PRhO angles = 90°; RhOC = 126°; OOC = 108°; OCC = 109°; CCRh = 115°; CRhO = 78.9°; HPRh = 109°; HCH = 109°. The P atoms are placed on the $+z$, $-x$, and $-y$ axes, Rh–O is along $+y$, and Rh–C approximately along $+x$.

Registry No. 2, 94324-89-7; 3, 94324-90-0.

(13) J. H. Ammeter, H.-B. Burgi, J. C. Thibeault, and R. Hoffmann, *J. Am. Chem. Soc.*, **100**, 3686 (1978).

Photoinitiated Intramolecular Hydrogen Transfer from Rhenium Polyhydrides to C_8 Cyclopolyolefins

Michaeleen C. L. Trimarchi, Mark A. Green, John C. Huffman, and Kenneth G. Caulton*

Department of Chemistry and Molecular Structure Center, Indiana University, Bloomington, Indiana 47405

Received July 16, 1984

The phototransient ReH_5P_2 (P ≡ PMe_2Ph), formed by photolysis of ReH_5P_3, reacts with cyclooctatetraene to give first $(\eta^4\text{-}C_8H_{10})ReH_3P_2$ as a stereochemically rigid complex of cyclooctatriene. This undergoes a thermal reaction at 25 °C to give $(\eta^5\text{-}C_8H_{11})ReH_2P_2$, shown to be a 1-5-$\eta^5$-cyclooctadienyl complex by NMR spectroscopy and X-ray diffraction. This complex has a piano stool form with a *diag*-ReH_2P_2 unit forming the base. The two hydride ligands lie *in* a mirror plane of the open pentadienyl ligand, and these hydrides are thus inequivalent; the spectral data show that this complex is stereochemically rigid. Analogous η^4-diene complexes are made from 1,5-cyclooctadiene and ReH_5P_3 (photochemically) and from ReH_7P_2 (thermally). Deuterium labeling experiments (employing ReD_5P_3 and C_8H_8) reveal that the transfer of three hydrides from metal to ring in the production of $(\eta^5\text{-}C_8H_{11})ReH_2P_2$ is regiospecific (i.e., no scrambling) and is wholly endo, consistent with an intramolecular mechanism. Crystallographic data (at −160 °C): orthorhombic, *Pbca* with $Z = 8$ and $a = 12.391$ (4) Å, $b = 17.882$ (6) Å, and $c = 20.441$ (8) Å.

Introduction

Irradiation ($\lambda > 300$ nm) of $ReH_5(PMe_2Ph)_3$ expels PMe_2Ph to convert this relatively unreactive saturated complex into the highly reactive transient species ReH_5P_2 (P ≡ PMe_2Ph).[1] This species will catalytically hydrogenate 1-hexene, but not 2-hexene. We have shown this is caused by the formation of a complex of the internal olefin which resists internal transfer of hydrogen from rhenium to the bound internal olefin: in the case of cyclopentene (C_5H_8), we isolate $ReH_3P_3(C_5H_8)$.[2] The stoichiometry of this complex is not simply that of an adduct of cyclopentene and the phototransient ReH_5P_2 but involves instead return of photodissociated phosphine. In an effort to understand this, we have explored the reactions of ReH_5P_2 with other olefins, particularly polyolefins. We report here that this approach gives products that are in fact hydrogen redistribution products derived from adducts of the olefin with ReH_5P_2.

(1) Green, M. A.; Huffman, J. C.; Caulton, K. G. *J. Am. Chem. Soc.* **1981**, *103*, 695.
(2) Green, M. A.; Huffman, J. C.; Caulton, K. G.; Rybak, W. K.; Ziolkowski, J. J. *J. Organomet. Chem.* **1981**, *218*, C39.

Experimental Section

Toluene, benzene, tetrahydrofuran, and diethyl ether were vacuum transferred from their solutions of sodium benzophenone ketyl. Hexane, pentane, and cyclohexane were vacuum distilled from sodium–potassium alloy. Benzene-d_6, toluene-d_8, and cyclohexane-d_{12} were dried over P_4O_{10} and vacuum distilled. Cyclooctatetraene was vacuum transferred at room temperature prior to use. Manipulations were performed in a N_2-filled Vacuum Atmospheres glovebox or on a Schlenk line equipped with a source of prepurified nitrogen.

Spectroscopy. Proton NMR spectra were recorded by using either a Varian T60 (at 35 °C), Varian HA-220 (at 16 °C), or Nicolet EM-360 (at 24 °C) spectrometer unless otherwise specified.

0276-7333/85/2304-0514$01.50/0